We are IntechOpen,
the world's leading publisher of
Open Access books
Built by scientists, for scientists

4,800
Open access books available

122,000
International authors and editors

135M
Downloads

154
Countries delivered to

Our authors are among the

TOP 1%
most cited scientists

12.2%
Contributors from top 500 universities

BOOK
CITATION
INDEX
CLARIVATE ANALYTICS
INDEXED

WEB OF SCIENCE™

Selection of our books indexed in the Book Citation Index
in Web of Science™ Core Collection (BKCI)

Interested in publishing with us?
Contact book.department@intechopen.com

Numbers displayed above are based on latest data collected.
For more information visit www.intechopen.com

5

Decay Heat and Nuclear Data

A. Algora and J. L. Tain
Instituto de Fisica Corpuscular, CSIC-Univ. de Valencia, Valencia
*Spain*

1. Introduction

The recent incidents at the Fukushima Daiichi nuclear power plant, following the great tsunami in Japan, have shown publicly, in a dramatic way, the need for a full knowledge and proper handling of the decay heat in reactors and spent-fuel pools.

In this chapter, after a short introduction to decay heat from the historical perspective we will discuss, how the decay heat is calculated from available nuclear data, and how the quality of the available beta decay data plays a key role in the accuracy and predictive power of the calculations. We will present how conventional beta decay experiments are performed and how the deduced information from such conventional measurements can suffer from the so-called pandemonium effect. Then we will introduce the total absorption technique, a technique that can be used in beta decay experiments to avoid the pandemonium effect. Finally, we will present the impact of some recent measurements using the total absorption technique, performed by an international collaboration that we lead on decay heat summation calculations and future perspectives.

1.1 The discovery of nuclear fission

In 1934 Fermi bombarded an uranium target with neutrons slowed down in paraffin in an attempt to produce transuranic elements. The first impression after the experiment was that uranium did undergo neutron capture and the reaction product was beta radioactive. Subsequent investigation of this reaction showed that the final activity produced included a range of different half-lives. This puzzle triggered intensive research from 1935 to 1939.

The identification of one of the activities produced as the rare-earth lantanum, first by Curie and Savitch in 1938 and then by Hahn and Strassmann in 1939, started to shed light on the puzzle. Indeed it was this fact that lead Hahn and Strassman to interpret the experimental activities as barium, lanthanum and cerium instead of radium, actinium and thorium. Shortly afterwards Meitner and Frisch (1939) suggested that the uranium nucleus, after the absorption of a neutron, splits itself into two nuclei of roughly equal size. Because the resemblance with the biological process in a living cell, the process was called fission. A typical example of the splitting is represented in Equation 1. Later measurements established the asymetric character of the process, the large energy release ($\sim$ 200 MeV) and the emission of prompt neutrons, which could trigger new fission processes and produce a chain reaction.

$$^{235}_{92}U +^1_0 n \rightarrow^{140}_{54} Xe +^{94}_{38} Sr + 2^1_0 n + \gamma + \sim 200 MeV \tag{1}$$
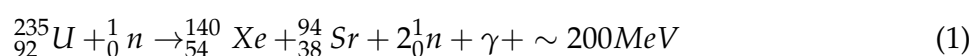
The first self-sustained chain reaction was achieved by Fermi in 1942 at the University of Chicago, which marked the begining of the nuclear age.

Since then many types of reactor have been developed for research, military and civil applications. Some examples include the Gas-Cooled reactor (GCR), Light Water Reactor (LWR), Heavy Water Reactor (HWR), Boiling Water Reactor (BWR), Liquid Metal Cooled Fast Breeder Reactor (LMCFBR) and so on. Independently of the kind of reactor one is considering there are important design and operating criteria which require a knowledge of the energy released in the decay of the fission products. In Table 1 an approximate distribution of the energy released in the fission of ^{235}U is presented. This table shows that from the total energy released inside the reactor (190 MeV), approximately 7 % is due to the beta decay of the fission products in the form of gamma and beta radiation. This source of energy is commonly called *decay heat* and depends on the fuel used in the reactor.

Distribution	MeV
Kinetic energy of light fission fragments	100
Kinetic energy of heavy fission fragments	67
Energy of prompt neutrons	5
Energy of prompt gamma rays	5
Beta energy of fission products	7
Gamma energy of fission products	6
Subtotal	190
Energy taken by the neutrinos	11
Total	201

Table 1. Approximate distribution of the energy released in the fission process of ^{235}U.

1.2 Decay heat

Once the reactor is shutdown, the energy released in radioactive decay provides the main source of heating. Hence, the coolant needs to be maintained after the termination of the neutron-induced fission process in a reactor. The decay heat varies as a function of time after shutdown and can be determined theoretically from known nuclear data. Such computations are presently based on the inventory of nuclei created during the fission process and after reactor shutdown, and their radioactive decay characteristics:

$$f(t) = \sum_i (\overline{E}_{\beta,i} + \overline{E}_{\gamma,i} + \overline{E}_{\alpha,i}) \lambda_i N_i(t) \tag{2}$$

where $f(t)$ is the power function, $\overline{E}_i$ is the mean decay energy of the ith nuclide (β, γ and α components), λ_i is the decay constant of the ith nuclide ($\lambda_i = ln(2)/T_{1/2,i}$), and $N_i(t)$ is the number of nuclide i at cooling time t. In the summation calculations 2, the first step is the determination of the inventory of nuclei $N_i(t)$, which can be obtained by solving a linear system of coupled first order differential equations that describe the build up and decay of fission products:

$$\frac{dN_i}{dt} = -(\lambda_i + \sigma_i \phi) N_i + \sum_j f_{j \to i} \lambda_j N_j + \sum_k \mu_{k \to i} \sigma_k \phi N_k + y_i F \tag{3}$$

where N_i represents the number of nuclides i, λ_i stands for the decay constant of nuclide i, σ_i is the average capture cross section of nuclide i, ϕ is the neutron flux, $f_{j \to i}$ is the branching ratio of the decay from nuclide j to i, $\mu_{k \to i}$ is the production rate of nuclide i per one neutron capture of nuclide k, y_i is the independent fission yield of nuclide i and F is the fission rate. These calculations require extensive libraries of cross sections, fission yields and decay data.

As mentioned earlier, an accurate assessment of the decay heat is highly relevant to the design of nuclear facilities. Consider for example the safety analysis of a hypothetical loss-of-coolant accident (LOCA) in a light water reactor or the cooling needs of a spent-fuel pool. Calculations of the decay heat are also important for the design of the shielding of discharged fuel, the design and transport of fuel-storage flasks and the management of the resulting radioactive waste. This assessment is obviously not only relevant to safety, it also has economic and legislative consequences. For example, the accuracy of the presently available decay data is still not high enough and this situation translates into higher safety margins implying greater economic costs. Reducing the uncertainty in available decay data is one of the main objectives of the work devoted to decay heat in present-day research.

Nowadays the most extended way to calculate the decay heat in reactors is the summation calculation method based on equations 2 and 3. As can be seen from 2 this method is simply the sum of the activities of the fission products produced during the fission process and after the reactor shutdown weighted by the mean decay energies. As a consequence, the summation calculation method relies heavily on the available nuclear data and this is the reason why in the early days of the nuclear age this method was not satisfactory. A different method, the so-called *statistical method* was the prefered way of evaluation of the decay heat at that time.

The statistical method was based on the work of Way and Wigner (Way & Wigner, 1948). They considered fission products as a sort of statistical assembly and relying on mean nuclear properties, they deduced empirical relations for the radioactive half-lives and atomic masses of fission products. With these relations the gamma (P_γ MeV/fission-s) and beta plus gamma (P_t MeV/fission-s) decay heat power functions in ^{235}U were determined as follows:

$$P_\gamma(t) = 1.26 t^{-1.2} \tag{4}$$

$$P_t(t) = 2.66 t^{-1.2} \tag{5}$$

These relations were considered valid for decay times t in seconds in the range of 10 seconds to 100 days. For many years this was the only available method for calculations of the decay heat. Other fissile materials were supposed to behave similarly to ^{235}U. This method is clearly simpler than the summation calculations, however it is incomplete by nature and less accurate for longer cooling times. In a natural way, with an increasing volume of nuclear data, the statistical method was gradually superseded by the summation calculations. Even though it is not used anymore, the work of Way and Wigner (Way & Wigner, 1948) was a seminal article, and the interested reader is encouraged to read it. Their predictions are approximatelly off by 60 % from todays accepted values, but the form of the parametrization of the decay heat as function $a \times t^{-b}$ is still used for benchmarks determination (benchmarks are obtained as a sum of functions of the form $a \times t^{-b}$ that cover the full cooling period, which are adjusted to experimental data).

It should be noted that in the beta part of equations 4 , 5 as well as in 2 the neutrino energy is not included.

2. Decay heat measurements

In the introduction we discussed how the decay heat can be calculated using two possible methods: the statistical method and via summation calculations, but any model for calculating the decay heat is only useful if it is able to describe properly experimental data. In this section we will discuss briefly how the decay heat can be measured and what benchmarks can be used to validate the calculations.

In general terms we can classify the decay heat measurements in two ways: a) radiation detection experiments and b) calorimetric experiments.

Radiation detection experiments consist of measuring the beta energy and the gamma energy coming from a small sample of fissile material that has been irradiated for a known length of time. In these measurements the aim is to increase the sensitivity of the setup for the particular goal of the study and reduce the sensitivity to any other type of radiation, which otherwise can lead to systematic errors. For example, in a beta energy measurement we will be prone to use a thin plastic detector, which has high efficiency for beta detection and a reduced efficiency for gamma rays. Conversely, in a gamma energy measurement one would use detectors of high efficiency for gamma rays and would try to avoid as much as possible the penetration of the betas in the gamma detection setup. Examples of these kinds of measurements can be seen in Refs. (Rudstam, 1990), (Dickens, 1981) and (Tasaka, 1988). These measurements have been also labelled in the past as "nuclear calorimetric" measurements, but the method itself is not truly calorimetric one, since it is only the detection of pure nuclear radiation with very high efficiency.

Real calorimetric experiments consist of absorbing the decay radiations and measuring the heat in the absorber. They follow well developed procedures that have been used extensively in studies of the energetics of chemical reactions. Many calorimetric measurements have been limited to intermediate cooling times, because of the difficulties of building an instrument that responds rapidly to changes in the power level, which is characteristic of short cooling times. Actually, for the application to the decay heat problem, the challenge is to build a calorimeter with a short time constant, or in other words to construct a setup that reacts quickly to the power release of the sample. Examples of such measurements can be found in the works of (Schrock, 1978) and (Yarnell, 1977).

There are several publications that summarize the efforts to improve the decay heat benchmarks covering different time periods. Some examples can be found in the reviews of Schrock (Schrock, 1979), Tobias (Tobias, 1980) and Tasaka (Tasaka, 1988). Nowadays the results of decay heat calculations are compared with the measurements of Akiyama *et al.* (Akiyama, 1982), Dickens *et al.* (Dickens, 1981), (Dickens, 1980) and Nguyen *et al.* (Nguyen, 1997). Decay heat benchmarchs can be found in the work of Tobias (Tobias, 1989), which is considered the standard in the field.

3. Nuclear data and beta decay

We will now concentrate on the data needs for summation calculations. Equation 3, which is the first step in the calculations requires a knowledge of decay constants, neutron capture cross-sections, decay branching ratios and independent fission yields. If this information is available, we can solve the coupled system of differential equations numerically or analytically and we will obtain the inventory of nuclei. The next step is to apply Eq. 2, which

requires the inventory of nuclei previously determined from 3, a knowledge of the decay constants and the mean energies released per decay. In this chapter we will concentrate on this last part of the problem: how the mean beta and gamma energies are determined from experimental data and what is the best technique to determine them.

Most nuclear applications involving beta decay rely on data available from databases, see for example the Evaluated Nuclear Structure Data file (ENSDF) (ENSDF, n.d.). The compiled data are typically the result of the evaluation of different measurements, using different techniques, but until now they have been mainly based on the use of Ge detectors (the technique that uses Ge detectors is conventionally called the high resolution technique, since Ge detectors have a very good energy resolution ($\Delta E / E \sim 0.15\%$)). In such experiments the main goal is to determine the levels populated in the decay (feeding probability to the different nuclear levels), as well as the quantum numbers that characterize the levels, since these data provide the basic nuclear structure information. As part of the analysis the level scheme populated in the decay, based preferably on $\gamma\gamma$ coincidence relations, should be constructed and its consistency should be tested using the intensity balance of gamma rays that populate and de-excite the different levels. Depending on the case, these experiments can suffer from systematic uncertainties.

3.1 The pandemonium effect

One example of systematic uncertainty is the so called pandemounium effect (Hardy, 1977), introduced by Hardy and coworkers in 1977. Pandemonium is the seat of Satan, where chaos reigns, in the epic poem *Paradise Lost* by John Milton, but in nuclear physics it has a very different meaning. Here pandemonium stands for the problems we face when constructing a complex level scheme from high resolution data in a beta decay experiment. The main difficulty is related to the relatively poor efficiency of the Ge detectors. Since building the level scheme is based on the detection of the individual gamma rays and on the detection of coincidences between them, if the detectors have poor efficiency we may not detect some of the gamma rays emitted in the de-excitation process of the populated levels. This means that the resulting level scheme is incomplete and the feeding pattern is incorrectly determined. Fig. 1 shows the effect of the pandemonium effect in a simplified level scheme.

We can explain the effect using the picture in Fig. 1. The left panel depicts the "real" situation in this simplified case. A schematic beta decay that goes 100 % of the time to level 2 is shown. Following the beta decay, level 2 in the daughter nucleus is de-excited by a cascade of two gamma rays (γ_1 and γ_2). In a beta decay experiment using Ge detectors the aim will be to detect the gamma rays de-exciting the populated levels and from the intensity balance of the gamma rays populating and de-exciting the levels in the daughter nucleus one will infer the beta feeding ($F = I_{out} - I_{in}$). So, in an ideal experiment one will infer that the feeding to level $F_2 = I_{\gamma_2} - 0$ is 100 % and $F_1 = I_{\gamma_1} - I_{\gamma_2}$ is 0 %. In such an experiment the detection setup will have an efficiency for detecting the individual gamma rays of ϵ_1 and ϵ_2 respectively and the probability of detecting coincidences will be proportional to the product $\epsilon_1\epsilon_2$. What happens if in reality the efficiency for detecting γ_2 is very small and we do not see this transition in our spectra and(or) we miss the coincidence relationship? We will detect only γ_1 and we will assign the feeding probability to level 1 ($F_1 = I_{\gamma_1}$). This means that instead of assigning the feeding to level 2 (real situation), we will have an apparent feeding of 100 % to level 1 and the nuclear structure information deduced will be incorrect. If this happens, we say that the

decay suffers from the pandemonium effect, but the real problem is that normally we do not know if the decay data suffers or not from the effect.
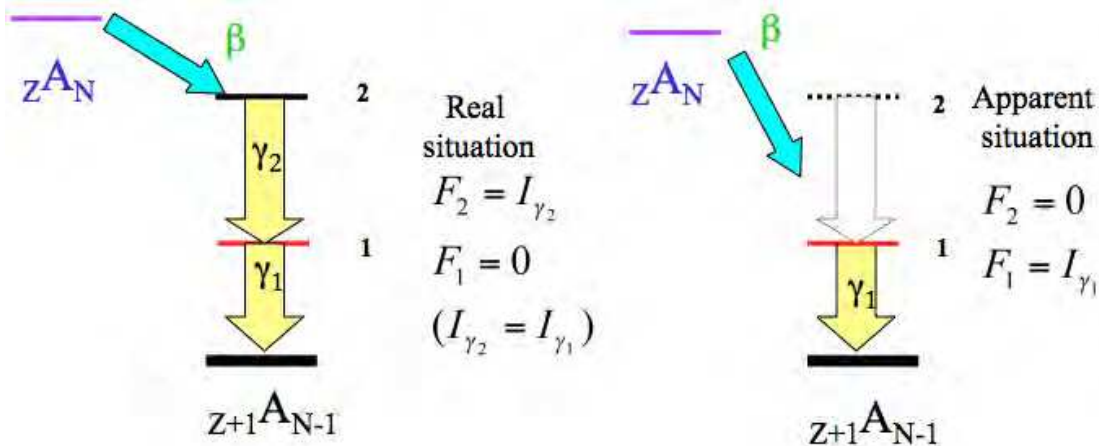

Fig. 1. Schematic decay to ilustrate the pandemonium effect. F represents the feeding (normalized to 100 %), which is determined from the intensity balance of gamma rays feeding and de-exciting the level and I_γ the gamma intensity.

Before entering into the details of how the pandemonium effect can be avoided it is worth to mention how the mean decay energies included in the summation calculations are determined. If we know the feeding probabilities ($f = F/100$) and the levels populated in the decay of nuclei i the mean γ and β energies released in the decay can be calculated according to the following:

$$\overline{E}_{\gamma,i} = \sum_j f_\beta(E_j) E_j \tag{6}$$

$$\overline{E}_{\beta,i} = \sum_j f_\beta(E_j) < E_{\beta j} > \tag{7}$$

where j runs over all levels fed in the daughter nucleus, $f_\beta(E_j)$ stands for the beta-feeding probability to level j, E_j is the excitation energy of level j in the daughter nucleus, and $< E_{\beta j} >$ is the mean energy of the beta particles emitted when feeding level j. This last quantity takes into account only the beta particle energies that feed the level j and does not include the energy taken away by the neutrinos. Since the betas have a continuous spectrum, $< E_{\beta j} >$ has to be calculated separately for each populated level j.

3.2 The total absorption technique

In the previous subsection it was assumed that to determine the feeding probability we depend on the detection of the gamma rays emitted following the beta decay. The main reason for this is that we cannot extract the feeding information easily from the detection of the beta particles. In a beta minus (plus) decay, the beta decay transition energy is shared between the beta minus (plus) particle, the recoiling nucleus and the anti-neutrino (neutrino). This means that if we measure the energy of the beta particles we do not have a discrete distribution, but a continuous one, in other words we are dealing with a three-body problem. Extracting information on the feeding probability from a continuous spectrum is not an easy task, which is why people prefer to work with the gamma-ray spectra associated with the beta decay. This situation is illustrated in Fig. 2 where again we show the ideal beta decay presented in Fig.
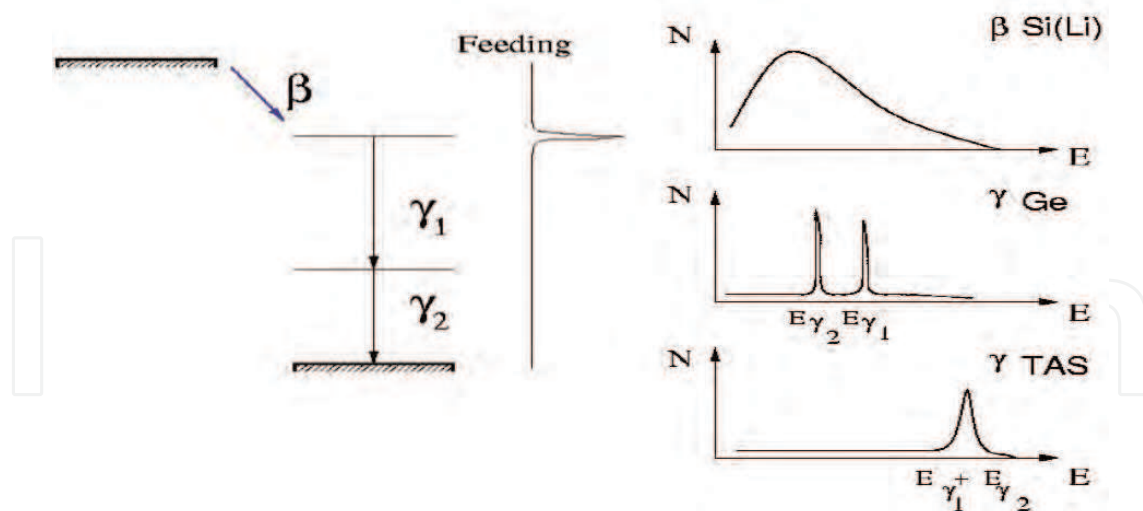
Fig. 2. Ideal beta decay seen by different detectors

1, but in this case we emphasize how the decay is seen by different detectors. The discrete nature of the gamma spectrum is what makes the problem tractable.

We have already discussed the pandemonium effect, which is related to the relatively low efficiency of the Ge detectors. If we have to rely on the detection of the gamma transitions then what can be done? It appears that the only solution is to increase drastically the gamma detection efficiency. In this way we arrive to the total absorption spectrometer (TAS) concept, which is presented in Fig. 3.

A TAS can be constructed using a large volume of detector material with high intrinsic efficiency for gamma rays, which surounds the radioactive source in a 4π geometry. In the left panel of Fig. 3 an ideal TAS is presented. There is also a change in the detection "philosophy" used in the TAS technique compared with high resolution (Ge detectors). Instead of detecting the individual gamma rays, the idea here is to detect the gamma cascades that follow the beta decay. So in principle, with an ideal TAS, the measured spectrum is proportional to the feeding probability of the decay. Now we can fully explain the rigth-hand panel of Fig. 2. What we see in the right panel is how the decay of the left panel is seen by different detectors. In the upper panel the betas detected by a Si detector are seen, which shows a continuous spectrum from which the beta feeding information is very difficult to extract if more levels are fed in the decay. The middle graph shows the individual gammas detected in an ideal high resolution (Ge) experiment, where the two individual gammas that follow the beta decay are detected. The lower graph shows how the decay is seen by an ideal TAS detector. In this case a spectrum is shown, which is proportional to the feeding pattern of the beta decay.

The left panel of Fig. 3 shows a photo of a real TAS, *Lucrecia*, which was installed by the Madrid-Strasbourg-Surrey-Valencia international collaboration at ISOLDE (CERN). It has a cylindrical geometry ($\varnothing$=h=38 cm), with a longitudinal hole perpendicular to the symmetry axis. The light produced in the NaI scintillator material by the detected radiation is read by eight photomultipliers. This photograph also shows the main reason why an ideal 100% efficient TAS can not be constructed. For the measurements we need to place the sources in the centre of the crystal, and to achieve this we need the telescopic tube that is seen in the foreground of the photograph. The hole, the dead material of the tube and of the tape transport system needed to take the sources to the centre of the detector makes the detector

less efficient. The second reason is that we would need very large detectors indeed to have a truly 100 % efficiency.
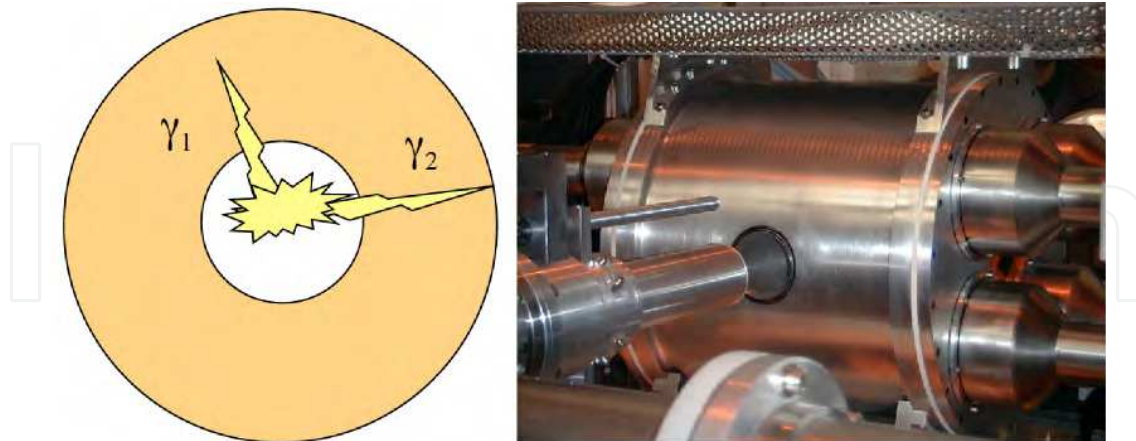

Fig. 3. Total absorption spectrometer. On the left panel an ideal TAS is presented, on the right a photo of the *Lucrecia* TAS installed at Isolde (CERN) can be seen.

The fact that we can not build a 100 % efficient detector makes the analysis of the TAS experiments difficult. To extract the feeding information we need to solve the following:

$$d = R(B)f \qquad (8)$$

where d represents the measured TAS spectrum (free of contaminants), $R(B)$ is the response matrix of the detector and f is the feeding distribution we would like to determine. In this equation B represents the branching ratios of the levels populated in the beta decay. We have developed algorithms and techniques that allow us to solve this problem. Because of their complexity we will not discuss them here in detail and the interested reader is encoraged to look at Refs (Tain, 2007; Cano, 1999). An example of a recent application of the technique, where details of how the analysis is performed, is presented in (Estevez, 2011). This recent work has implications for neutrino physics.

3.3 Pandemonium and decay heat

As mentioned earlier, to calculate the mean energies the feeding probability to the different levels populated in the decay is needed (Eqs. 6, 7). Now we can understand why TAS measurements can have an impact and should be applied to decay heat studies. If we have a beta decay that suffers from the pandemonium effect, the mean gamma energies will be underestimated and the beta energies will be overestimated. This is shown schematically in Fig. 4. Since the application of the TAS technique is the only way to avoid the pandemonium effect, this technique should be used for studying decays that are important for the decay heat problem.

Our interest in the decay heat topic was triggered by the work of Yoshida and coworkers (Yoshida, 1999). At the begining of the 1990s one of the most successful data bases for summation calculations was the JNDC-V2 (Japanese Nuclear Data Committee version 2) database. In this database the gross theory of beta decay (Takahashi & Yamada, 1969) was used to supplement experimental data that might suffer from the pandemonium effect. For example in (Tasaka, 1988) it is mentioned that the mean energies of many decays having a beta
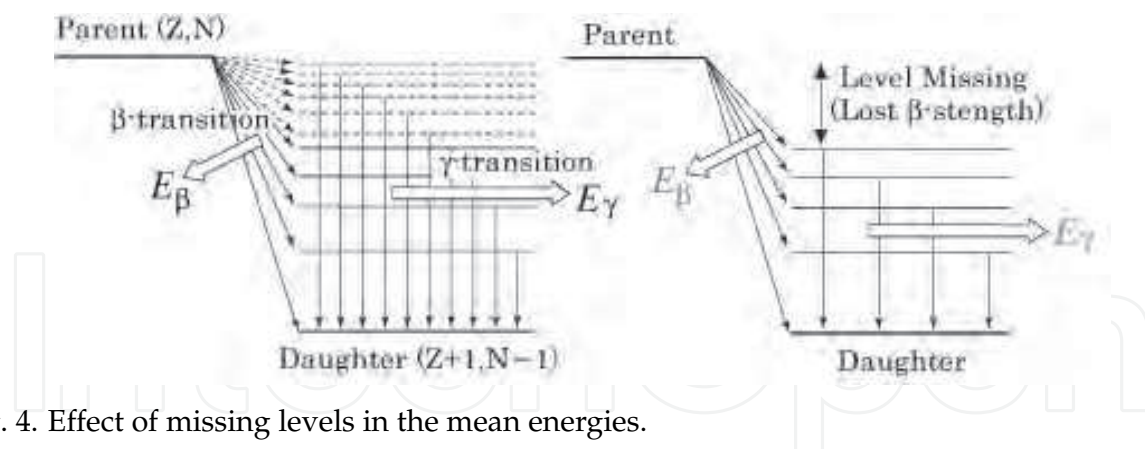
Fig. 4. Effect of missing levels in the mean energies.

decay Q value larger that 5 MeV were supplemented by theoretical values calculated using the gross theory. Even though the database in general worked well for the gamma component of the ^{239}Pu decay heat, there was a significant remaining discrepancy in the 300-3000 s cooling time. Yoshida studied the possible causes for the discrepancy and proposed several possible explanations. The most plausible was the possibility that the decay energies of some nuclides with half-lives in the range of 300-3000 s or with precursors with similar half-lives suffered from the pandemonium effect. After a careful evaluation of possible candidates he proposed that the decays of $^{102,104,105}Tc$ should be measured with the total absorption technique.

In the process of defining priorities for the TAS measurements related to decay heat, contact with specialists in the field was established and a series of meetings were held under the auspices of the International Atomic Energy Agency (IAEA). As a result of these meetings a list of nuclei that should be measured with the total absorption technique was defined (Nichols, 2007). This list included the Yoshida cases ($^{102,104,105}Tc$) and some additional nuclei (in total 37). The nuclei were identified based on their contribution to the decay heat in different fuels, and in order to reduce the discrepancies between the major international databases (JENDL (Shibata, 2011), JEFF (Kellett, 2009), ENDF (Chadwick, 2006)). Additionally, this list included some cases that deserve to be measured for other reasons. For example there are TAS measurements that were performed in the past by Greenwood and coworkers (Greenwood, 1992). These TAS measurements were analyzed using different procedures from those used nowadays. It is important to verify the results and compare them with new measurements using different analysis techniques to look for systematic uncertainties. Similarly the measurements of (Rudstam, 1990), obtained from direct spectral measurements can be checked against TAS measurements (Tain & Algora, 2006).

4. Experiments and experimental techniques

We have started a research programme aimed at the study of nuclei included in the list of the WPEC-25 group of the IAEA (Nichols, 2007). To perform a succesful experiment, the first step is to define the best facility to carry it out. In recent years there have been extensive developments in the methods used to produce radioactive beams. Indeed, we are living a period of renaissance and renewal for these facilities, since new ones have been constructed and others are under development, construction and upgrade (FAIR, HIE-ISOLDE, HRIBF, etc.). In essence these facilities are based on two main methods of producing radioactive beams, the ISOL method and the fragmentation or In-Flight method. In the ISOL technique an intense particle beam, impinges on a thick target. After diffusion and effusion, the radioactive

nuclei produced are mass selected, ionized and re-accelerated in a post-accelerator. This method in general produces cleaner nuclear species, but requires specific developments of the ion sources, which involve chemistry and physics aspects. Its major constrain is related to the production of very short-lived isotopes and the production of beams of refractory elements that are difficult to extract from ion sources. The fragmentation technique, as the name implies, is based on the fragmentation of high energy projectiles on target nuclei and the subsequent separation and selection in-flight of the radioactive nuclei produced using magnetic spectrometers. With this technique it is possible to study very short-lived isotopes, but typically the nuclei are produced in a less clean enviroment. In this case the experiments rely on the identification of the nuclear species produced on an ion-by-ion basis.

Some of the nuclei included in the WPEC-25 list are refractory elements, so it was not possible to produce them in "conventional" ISOL facilities such as ISOLDE(CERN). So for our experiments we decided to use the Ion-Guide Isotope Separator On-Line (IGISOL) facility of the University of Jyväskylä (Äystö, 2001). In this facility the ion guide method was developed, which can be considered to be a "chemistry" independent ISOL method (Dendooven, 1997). The working principle of the ion guide method is that the radioctive nuclides are produced in a thin target after bombarment with the accelerator beam. The reaction products (recoils) fly out of the target and are transported by a differential pumping system to the first stage of the accelerator. The mean path of the recoils is optimized in such a way that they survive as singly charged ions. By this method we obtain a system, which is chemically insensitive and very fast (ms). A schematic picture of the ion-guide principle is presented in Fig. 5.
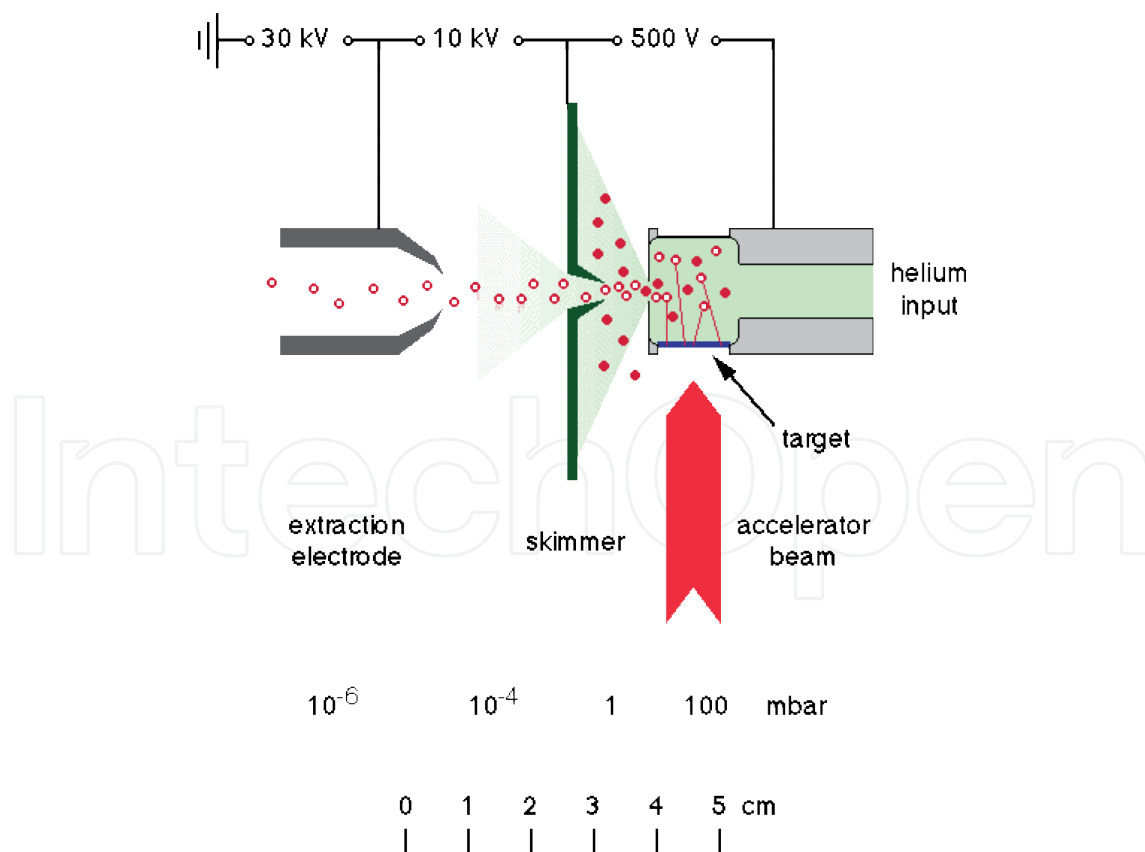

Fig. 5. The ion guide principle.

At the IGISOL facility several ion guides were developed. For our experiments we used a fission ion guide, which allows the extraction of fission products produced in proton-induced fission. This was the chosen method for the production of the radioactive nuclides of interest. Following the extraction, the ions can be separated using a dipol magnet. The magnetic field of the dipol bends the ions to different trajectories depending on their charge-to-mass ratio. Since most of the ions come out of the ion guide singly charged, mass separation is achieved. To characterize the separation quality, the mass resolving power of the system is used, which is a measure of how well species with different masses are separated ($\Delta m/m$). At IGISOL the mass resolving power typically varies from 200 to 500, depending on the experimental conditions. This is not enough to separate ions that have the same mass number (isobars), but it is adequate to separate isotopes of the same element. That is why the instrument is called an isotope separator. For the TAS measurements this separation is not enough, since you can have several isobars produced in fission that can not be separated with the isotope separator, and their decay will appear as contaminants in the TAS spectrum. An advantage of the IGISOL facility is that a Penning trap system (JYFLTRAP) (Kolhinen, 2004) can be used for further isobaric separation. Penning traps are devices for the storage of charged particles using a homogeneous static magnetic field and a spatially inhomogeneous static electric field. This kind of trap is particularly well suited for precision mass spectroscopy, but they can also be used as high resolution separators for "trap-assisted" spectroscopic studies as in our experiments.
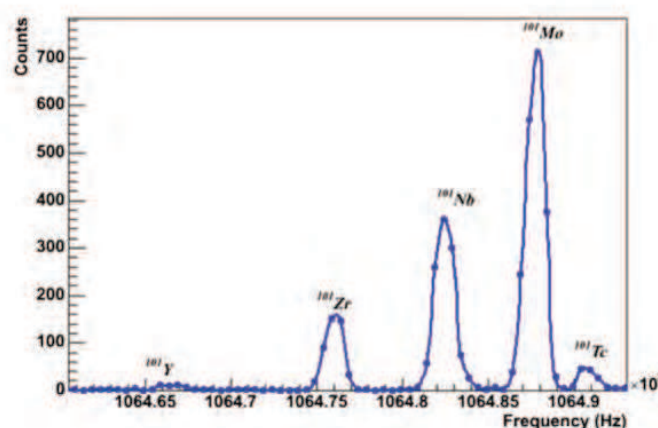

Fig. 6. Mass scan in the Penning trap for A=101 fission products. During the experiment the frequency corresponding to the isotope of interest is set in the trap, and then a very pure beam can be used for the measurements.

With a Penning trap system a mass resolving power of the order of 10^5 and even 10^6 can be achieved. The good separation is shown in Fig 6, where a frequency scan in the Penning trap for mass A= 101 prior to one of our experiments is presented. Once a frequency in the trap is set for a particular isobar, a very pure radioactive beam can be obtained. The only disadvantage of this system is the relatively low intensity of the ion beam, since the transmission of the trap is only a few percent.

Figure 7 shows an schematic picture of the setup used in our experiments in Jyväskylä. In this setup the radioactive beam coming from the trap is implanted in a tape system that allows us to transport the radioactive sources to the measuring position and to remove the undesired daughter activities. The cycles of the tape are optimized according to the half-life of the isotope of interest.
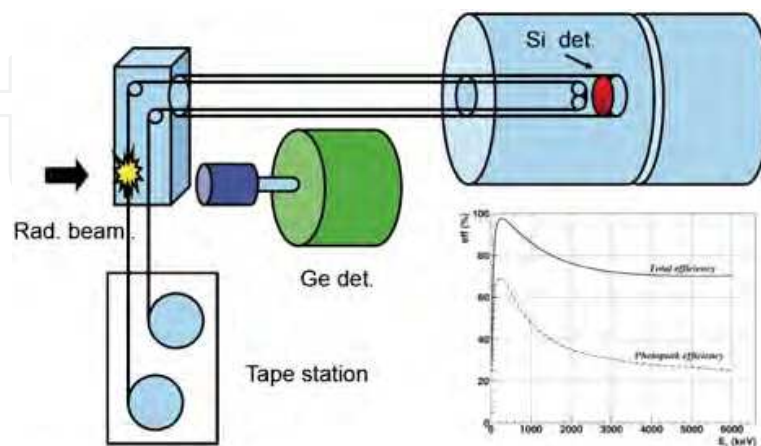

Fig. 7. Schematic picture of our experimental setup at IGISOL for TAS measurements. In the inset the peak and total efficiency of the used TAS is presented.

4.1 First trap assisted TAS experiment

At IGISOL we have performed two trap-assisted TAS experiments related to the decay heat problem. Here we will discuss briefly the first experiment and its impact. The second experiment is presently in the analysis phase. It is worth noting that in the second experiment we have used for the first time a segmented BaF_2 TAS detector which additionally provides information on the multiplicity of the gamma cascades following the beta decay. This extra information is useful for the analysis of the complex beta decay data.

The analysis of a TAS experiment is a lengthy procedure and requires several stages. The first phase requires a careful evaluation of the contaminants and distortions of the measured spectrum in order to determine d. Then the calibration of the experimental data in energy and width and a precise characterization of the TAS detector using Monte Carlo (MC) techniques is

Nuclide	$T_{1/2}$ s	$\overline{E_\gamma}$ ENDF	$\overline{E_\gamma}$ TAGS	$\overline{E_\beta}$ ENDF	$\overline{E_\beta}$ TAGS
^{101}Nb	7.1(3)	270(22)	445(279)	1966(307)	1797(133)
^{105}Mo	35.6(16)	552(24)	2407(93)	1922(122)	1049(44)
^{102}Tc	5.28(15)	81(5)	106(23)	1945(16)	1935(11)
^{104}Tc	1098(18)	1890(31)	3229(24)	1595(75)	931(10)
^{105}Tc	456(6)	668(19)	1825(174)	1310(205)	764(81)
^{106}Tc	35.6(6)	2191(51)	3132(70)	1906(67)	1457(30)
^{107}Tc	21.2(2)	515(11)	1822(450)	2054(254)	1263(212)

Table 2. Comparison of mean gamma and beta energies included in the ENDF/B-VII database with the results of the analysis of our measurements (in keV).

required. For the MC simulations the GEANT4 code (Agostinelli, 2007) is used. In this phase a careful characterization of the setup is performed until measurements with conventional radioactive sources like ^{24}Na, ^{137}Cs and ^{60}Co are very well reproduced by the MC code. Once this has been achieved, the response function of the detector to the decay of interest can be calculated. This requires the definition of the level scheme that may be populated in the decay (B or branching ratio matrix). To construct the branching ratio matrix we take into account known levels up to a certain excitation in the daughter (E_{cut}) and above that cut-off energy we use a statistical model to generate levels and their branchings. The information on the low-lying levels and their branchings is taken from conventional high resolution measurements, because this information is correct in general if available (known levels). For the statistical model we use a back shifted Fermi formula for the level density and gamma strength functions, which define the probabilities that gamma rays connect the different levels (known and unknown part). Once the B is determined, the $R(B)$ is calculated from the MC responses of the detector to the different γ and β transitions and 8 is solved. As part of the analysis, the cut-off energy, the accepted low-lying levels and the parameters of the statistical model are changed if necessary. The final result of the analysis is a feeding distribution, from which nuclear structure information can be obtained in the form of the beta strength distribution (S_β), and in the case of the decay heat application mean beta and gamma energies can be calculated (6 and 7).

The impact of our first experiment can be seen in Table 2, where the mean energies of the ENDF database are compared with the results of our measurements. From this table the relevance of performing experiments is also clear. Two nuclei (^{101}Nb, ^{102}Tc), that were suspected to suffer from the pandemonium effect did not, even though they have large Q_β decay values. The remaining nuclei all suffered from the effect (see for example the large increase in the mean gamma energy and the reduction in the mean beta energy with respect to high resolution measurements for ^{104,105}Tc). In Fig. 8 the results for the gamma component of ^{239}Pu are presented. They are compared with ENDF (ENSDF, n.d.) before and after the inclusion of our new data (Sonzogni, n.d.). Similar conclusions have been obtained recently using the JEFF database (Mills, n.d.). The new TAS results were published in (Algora, 2010).
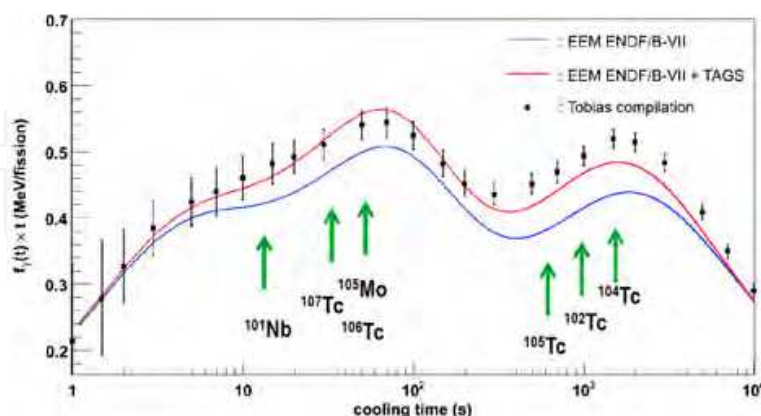

Fig. 8. Comparison of the summation calculations for the gamma component of the decay heat in ^{239}Pu. The experimental points with errors are taken from the Tobias compilation (Tobias, 1989). The blue line represent the results obtained using the ENDF data base without the inclusion of the new results (Algora, 2010). The red line represents the results after the inclusion of the new TAS measurements. The cooling time at which the contribution of the measured nuclei is maximal is represented by arrows.

As a result of our measurements, a large part of the discrepancy pointed out by (Yoshida, 1999) in the 300-3000 s cooling interval and additionally the discrepancy at low energies has been solved within the ENDF database. The new data were also used to perform summation calculations for the gamma component of ^{235}U. In this case the results were disappointing. Our new results had very little impact. This can be understood in terms of the cummulative fission yields of the nuclei in question. They sample approximatelly 33.8 % of the fission in ^{239}Pu, but only 13.5 % in ^{235}U. Additionnally from the 13.5 % in ^{235}U, ^{101}Nb, ^{102}Tc amounts to 9.2 %, which does not bring a large change in the mean energies. This explains why our measurements to date can only represent a relative change of approximatelly 4.3 % in ^{235}U, compared to the 22.6 % relative impact in ^{239}Pu with respect to the earlier values of the ENDF database.

5. Conclusions and outlook

In this chapter we have described how total absorption measurements can play an important role in improving the beta decay data necessary for summation calculations. We have discussed the technique and how its combination with IGISOL and the JYFL Penning trap has allowed us to perform measurements that had a large impact in the decay heat of ^{239}Pu. These measurements can also be relevant for other reasons. The beta feeding distributions can also be used to deduce the beta strength and test nuclear models. This region (nuclear mass ~ 100) is interesting from the point of view of nuclear structure. For example it has been suggested that triaxial shapes play a role in this region of the nuclear chart (Möller, 2006). Most known nuclei have prolate (rugby ball shape) or spherical shapes in their ground state. If triaxiality plays a role in the structure of these nuclei, this will afect the distribution of the strength in the daughter and it may be studied using the TAS technique. Actually, we have previously used the TAS technique to infer shape effects in the A ~ 70 region (Nacher, 2004) and have started recently a related research programme in the lead region (Algora, 2005).

We plan to continue to make measurements using the TAS to obtain data of relevance to decay heat, but it is important to mention that there also similar efforts ongoing in other facilities and by other groups. In Argonne National Laboratory (Chicago, USA), there is a new facility under construction *CARIBU*, that will allow for the production of neutron-rich species from the fission of ^{252}Cf. Here there are plans to use again the TAS detector employed in the measurements of Greenwood (Greenwood, 1992) and coworkers. Another example is the development of the MTAS detector by the group of Rykaczewski and coworkers, that will be used at the HRIBF facility at Oak Ridge (USA). These new facilities will contribute in the future to improving the quality of beta decay data for the decay heat application.

Our work had a large impact in ^{239}Pu, but there is still a large amount of work to be done for ^{235}U as was mentioned in the previous section. Additionally decays relevant for other fuels like ^{232}Th should be also studied. Recent work by Nichols and coworkers has identified which nuclei should be measured for the ^{232}Th fuel (Gupta, 2010).

Another aspect worth mentioning is the possible impact of these measurements in the prediction of the neutrino spectrum from reactors. In the same fashion as beta and gamma summation calculations are performed, neutrino summation calculations can be done for a working reactor. Because of the very small interaction cross section, neutrinos leave the reactor almost without interaction in the core. They carry information on the fuel composition and on the power level and their flux can not be shielded or controlled. Because of the small

interaction cross section with matter they are difficult to detect ($\sim 10^{-43} cm^2$), but they are produced in very large numbers from the fission products. For example, approximately six antineutrinos are produced per fission, and a one GW_{el} reactor produces of the order of 10^{21} neutrinos every second. The precision of the neutrino spectrum measurements can be important for neutrino oscillation experiments in fundamental physics experiments like Double CHOOZ and for non-proliferation applications (Fallot, 2007). There is presently a working group of the IAEA, which studies the feasibility of building neutrino detectors, which if positioned outside and close to a nuclear reactor can be used to monitor the power level and the fuel composition of the reactor. These measurements, if they reach the necessary precision, can be used to indicate the fuel used and to monitor manipulations of the fuel in a non-intrusive way (Porta & Fallott, 2010). We plan future measurements to address this topic of research.

6. References

K. Way and E. Wigner, Phys. Rev. 73 1318 (1948)

G. Rudstam *et al.*, Atom. Dat. and Nucl. Dat. Tabl. 45, 239 (1990)

J. K. Dickens *et al.*, Nucl. Sci. Eng, 78, 126 (1981)

K. Tasaka, J. Katakura, T. Yoshida, Nuclear Data for Science and Technology (1988 MITO), p 819-826, 1988

V. E. Schrock *et al.* EPRI Report, NP616, Vol. 1, 1978

J. L. Yarnell and P. J. Bendt, Los Alamos Scientific Laboratory Report, LA-NUREG-6713, 1977

V. E. Schrock, Progress in Nucl. Energy, Vol. 3. pp. 125-156, 1979

A. Tobias, Progress in Nucl. Energy, Vol. 5. pp. 1-93, 1980

K. Tasaka, J. Katakura, T. Yoshida, Nuclear Data for Science and Technology (1988 MITO), p 819-826, 1988

M. Akiyama, S. An, Proc. Int. Conf. on Nuclear Data for Science and Technology, Antwerp, p. 237, 1982 and references therein

J. K. Dickens *et al.*, Nucl. Sci. Eng 74, 106, (1980)

H. V. Nguyen *et al.*, Proc. Int. Conf. on Nucl. Data for Science and Technology, Triestre, p. 835 (1997)

A. Tobias, CEGB Report No. RD/B/6210/R89, 1989

http://www.nndc.bnl.gov/ensdf

J. C. Hardy *et al*, Phys. Letts 71B (1977) 307.

J. L. Tain, D. Cano-Ott, Nucl. Instrum. and Meth. Phys. Res. A 571 (2007) 728 and 719.

D. Cano-Ott *et al.*, Nucl. Instrum. and Meth. Phys. Res. A 430 (1999) 488 and 333.

E. Estevez *et al.*, Phys. Rev. C 84 (2011) 034304

T. Yoshida *et al*, J. Nucl. Sci. and Tech. 36 (1999) 135.

K. Takahashi, M. Yamada, Prog. Theor. Phys. 41 (1969); K. Takahashi, Prog. Theor. Phys. 45 (1971) 1466; T. Tchibana, M. Yamada, Y. Yoshida, Prog. Theor. Phys. 84 (1990) 641

A. Nichols, NEA report NEA/WPEC-25 (2007) 1.

K. Shibata *et al.*, J. Nucl. Sci. and Tech. 48 (2011) 1; K. Shibata *et al.*, J. Nucl. Sci. and Tech. 39 (2002) 1125

M. A. Kellett, *et al.*, JEFF Report 20, OECD 2009, NEA No. 6287; A. J. Koning *et al.*, Proc. of the Int. Conf. on Nucl. Data for Science and Technology, Nice, 2007

M. B. Chadwick *et al.*, Nucl. Data Sheets 107 (2006) 2931

R. C. Greenwood *et al.*, Nucl. Instrum. and Meth. Phys. Res. A 390 (1997) 95, Nucl. Instrum. and Meth. Phys. Res. A 314 (1992) 514

J. L. Tain, A. Algora, IFIC-06-1 Report, 2006

J. Äystö, Nucl. Phys. A 693 (2001) 477.

P. Dendooven, Nucl. Instrum. Meth. Phys. Res. B 126 (1997) 182

V. Kolhinen et al., Nucl. Instrum. Methods Phys. Res., Sect. A 528 (2004) 776

S. Agostinelli *et al*, Nucl. Instrum. and Meth. Phys. Res. A 506 (2003) 250.

A. Sonzogni, private communication

A. Algora *et al*, Phys. Rev. Letts. 105 (2010) 202501; D. Jordan, PhD thesis, Valencia, 2010; D. Jordan *et al*, in preparation

R. W. Mills, private communication

P. Möller *et al*, Phys. Rev. Letts. 97, 162502 (2006)

E. Nacher *et al*, Phys. Rev. Lett. 92, 232501 (2004)

A. Algora *et al*, ISOLDE Experimental Proposal IS440, CERN-INTC-2005-027, INTC-P-199

M. Gupta *et al*, INDC(NDS)-0577

M. Fallot *et al*, Proceedings of the Int. Conf. on Nucl. Data for Science and Technology 2007, p. 1273.

A. Porta, M. Fallott, JEFF Meeting 2010 and private communication.
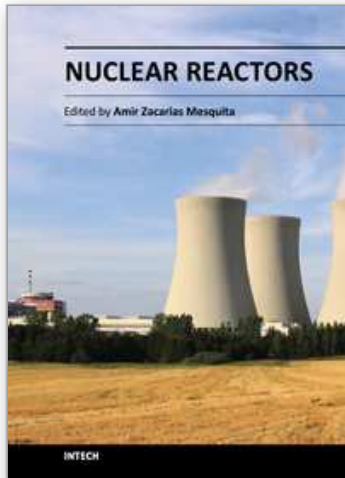
Nuclear Reactors

Edited by Prof. Amir Mesquita

This book presents a comprehensive review of studies in nuclear reactors technology from authors across the globe. Topics discussed in this compilation include: thermal hydraulic investigation of TRIGA type research reactor, materials testing reactor and high temperature gas-cooled reactor; the use of radiogenic lead recovered from ores as a coolant for fast reactors; decay heat in reactors and spent-fuel pools; present status of two-phase flow studies in reactor components; thermal aspects of conventional and alternative fuels in supercritical water?cooled reactor; two-phase flow coolant behavior in boiling water reactors under earthquake condition; simulation of nuclear reactors core; fuel life control in light-water reactors; methods for monitoring and controlling power in nuclear reactors; structural materials modeling for the next generation of nuclear reactors; application of the results of finite group theory in reactor physics; and the usability of vermiculite as a shield for nuclear reactor.

INTECH
open science | open minds